

GRAIN BOUNDARY EVOLUTION: NEW PERSPECTIVES

M. EMELIANENKO*, D. GOLOVATY†, D. KINDERLEHRER‡, AND S. TA'ASAN§

Abstract. In this paper, we study mesoscopic behavior of a grain boundary system and investigate the possibility of modeling texture evolution. One of the most challenging aspects of this problem is to understand the role of topological reconfigurations during coarsening. To this end, we investigate grain boundary evolution in a one-dimensional system designed specifically to target critical event evolution in microstructure. We suggest stochastic frameworks that may be used to model this system. We compare the predictions of the models with simulations and discuss their limitations and possible extensions to higher-dimensional cases.

1. Introduction. Most technologically useful materials arise as polycrystalline microstructures, composed of myriads of small crystallites, called grains, separated by their interfaces, called grain boundaries. The energetics and connectivity of the network of boundaries are implicated in many properties across wide scales, for example, functional properties, like conductivity in microprocessors, and lifetime properties, like fracture toughness in structures. Preparing arrangements of grains and boundaries suitable for a given purpose is a central problem in materials science. It likewise presents many challenges for mathematical modeling, simulation, and analysis. Historical emphasis here has been on the geometry, or more exactly, on statistics of simple geometric features of experimental and simulated polycrystalline networks. We are now turning our attention to texture, the mesoscopic description of arrangement and properties of the network described in terms of both geometry and crystallography.

There is a great wealth of experimental work available concerning texture in polycrystalline systems: it has, after all been of recognized importance since the stone age [1]. In recent years, we have witnessed a changing paradigm in the materials laboratory with the introduction of automated data acquisition technologies. This has permitted the collection of statistics on a vast scale and their use to optimize aspects of material behavior. There are situations, for example, where it is possible to quantify the amount of alignment or misalignment sufficient to produce a corrosion resistant microstructure. To rise beyond this level of anecdotal observation, the thermodynamics of the material system must be related to texture and texture related properties. Said in a different way, are there any texture related distributions which are material properties? Some geometric features of the configuration, like relative area statistics have these properties in the sense that they are robust but they are not strongly related to energetics. Recent work has provided us with a new statistic, the grain boundary character distribution, which has enormous promise in this direction. The grain boundary character distribution is a measure of relative amount of grain boundary with a given net misorientation. Owing to our new ability to simulate the evolution of large scale systems, we have been able to show that this statistic is robust and, in elementary cases, easily correlated to the grain boundary energy (see [7], [8]).

We stress, however, that the mechanisms by which the distribution develops

*Department of Mathematical Sciences and Center for Nonlinear Analysis, Carnegie Mellon University, Pittsburgh, PA 15213 email: masha@cmu.edu.

† Department of Theoretical and Applied Mathematics, The University of Akron, Akron, OH 44325, email: dmitry@math.uakron.edu.

‡ Department of Mathematical Sciences, Carnegie Mellon University, Pittsburgh, PA 15213, email: davidk@cmu.edu.

§ Department of Mathematical Sciences, Carnegie Mellon University, Pittsburgh, PA 15213, email: shlomo@andrew.cmu.edu.

from an initial population are not yet understood. As a polycrystalline configuration coarsens, facets are interchanged and some grains grow larger and others disappear. These critical events determine the evolution of our distribution. This is because the system coarsens by the motion of the triple junctions, with low energy boundaries sweeping out those of higher energy. The triple junction population, in turn, is determined by the critical events. The regular evolution of the network is governed by the Mullins Equations of curvature driven growth introduced in [2],[3],[4], supplemented by the Herring Condition force balance at triple junctions, a system of parabolic equations with complementing boundary conditions, as shown in [5] and [6]. Some of the most popular theories based on these results are summarized in [9] and [10]. The critical events, on the other hand, have not yet received such an extensive treatment, while they play a very important role in the interface evolution.

The major difficulty in developing a theory of the grain boundary character distribution lies in the lack of understanding of these stochastic events. In this work we concentrate our effort on the mechanisms governing these processes. Here we shall investigate a simplified 1-dimensional model that serves as a surrogate, exhibiting the main features of the interacting grain boundary network. In this model, we shall have boundaries and junctions between boundaries moving under a form of gradient flow. It is introduced precisely in the section 2.

There are several approaches one might adopt to describe the behavior of the grain boundary character density, from purely deterministic to stochastic. In a recent paper ([11]), we present a statistical model for critical events from the point of view of fractional continuous time random walks and show its relation to the stochastic Poisson type equations. Here we focus our attention on the strategies inspired by statistical theory of gases. Motivated by the apparent presence of stationary distributions resulting from the statistical analysis of such a system as described in section 3, we consider several theoretical frameworks capable of describing it. In section 4 we look at the evolution of boundaries based on associated orientation parameters. We propose several Fokker-Planck and birth-death type of equations to model early stages of the process with some success. The advantage of this approach is its low complexity and ability to successfully model the initial stages of the evolution. A framework based on statistical mechanics is introduced in section 5 to remedy some drawbacks of the previous approach. We construct a Boltzmann-type equation modeling grain interaction which can successfully reproduce simulation data with the adequate choice of parameters and has a good potential for generalization to higher dimension. In fact, it appears that this approach can yield even better results in 2D due to the restrictions that 1-dimensional problem poses on grain interactions, in contrast to its visual simplicity. We show that both short and long time behavior of the system can be completely recovered by introducing an extended set of parameters. The analysis of the role played by the nearest neighbor dependence on the dynamics of critical events that we identified in this study sheds a new light on the discussion of interface driven growth in general.

The purpose of this paper is to summarize some of the numerical observations and theoretical approaches associated with this kind of systems. We propose the birth-death and Boltzmann type theories that have a potential for successfully describing each stage of the grain growth dynamics in the higher dimensional systems.

2. Model description. To construct our one dimensional model, consider intervals $[x_i, x_{i+1}]$, $i = 0, \dots, n$, on the line, which may vary in time, where, for simplicity, we assume the periodicity condition $x_0 = x_n$. For each interval $[x_j, x_{j+1}]$, choose

a number α_j from the set $\{\alpha_i\}_{i=1,\dots,n}$. The intervals $[x_j, x_{j+1}]$ are viewed as grain boundaries and the points x_j correspond to triple points. The parameters $\{\alpha_i\}_{i=1,\dots,n}$ represent orientations in some sense. $l_j = x_{j+1} - x_j$ is the length of the j^{th} grain boundary. Now choose a non-negative potential $f(\alpha)$ and define the energy

$$En(t) = \sum f(\alpha_i)(x_{i+1}(t) - x_i(t)) \quad (2.1)$$

Consider the gradient flow dynamics characterized by the system of ordinary differential equations

$$\dot{x}_i = f(\alpha_i) - f(\alpha_{i-1}), \quad i = 0, \dots, n. \quad (2.2)$$

The parameter α_i is prescribed for each grain boundary initially according to some random distribution and does not change during its lifetime. The velocities of the grain boundaries can be computed from the relation

$$v_i = \dot{x}_{i+1} - \dot{x}_i = f(\alpha_{i+1}) + f(\alpha_{i-1}) - 2f(\alpha_i) \quad (2.3)$$

Notice that the velocities remain constant until the moment a neighboring grain boundary collapses, at which instant a jump of the velocity occurs. Every such critical event changes the statistical state of the model through its effect on the grain boundary velocities and therefore affects further evolution of the grains. Notice that the lengths of the individual grain boundaries vary linearly between the corresponding jump events and depend entirely on the corresponding grain boundary velocities.

An important feature of the thermodynamics of grain growth is that it is dissipative for the energy during normal grain growth. We will now show that the model introduced above is in fact a precise analogy of the system of grain boundaries, including the dissipative behavior throughout its lifetime. At critical events, the algorithm is designed to enforce dissipation. We check that (2.2) is also dissipative. First consider a time t when there is no critical event. Then

$$\begin{aligned} \frac{dEn}{dt}(t) &= \sum f(\alpha_i)v_i \\ &= \sum f(\alpha_i)(f(\alpha_{i+1}) - f(\alpha_i) - f(\alpha_i) + f(\alpha_{i-1})) \\ &= \sum f(\alpha_i)(f(\alpha_{i+1}) + f(\alpha_{i-1}) - 2\sum f(\alpha_i)^2) \\ &\leq 2(\sum f(\alpha_i)^2)^{\frac{1}{2}}(\sum f(\alpha_i)^2)^{\frac{1}{2}} - 2\sum f(\alpha_i)^2 \\ &= 0 \end{aligned}$$

by periodicity and the Schwarz Inequality. Now suppose that the grain boundary $[x_c, x_{c+1}]$ vanishes at time $t = t_{crit}$ and, for simplicity, it is the only vanishing grain boundary. Then the velocity of that boundary $v_c(t) < 0$, $t < t_{crit}$, namely,

$$\frac{1}{2}(f(\alpha_{c+1}) + f(\alpha_{c-1})) < f(\alpha_c).$$

and $l_c \rightarrow 0$ for $t \rightarrow t_{crit}^-$. Now

$$En(t) > \sum_{i \neq c} f(\alpha_i)l_i, \quad t < t_{crit},$$

and

$$En(t_{crit}) = \lim_{t \rightarrow t_{crit}} \sum_{i \neq c} f(\alpha_i) l_i \leq \lim_{t \rightarrow t_{crit}} En(t)$$

and we have checked that the model system is dissipative.

From the materials science perspective, it is important to know the distributions of relative lengths, as well as grain boundary orientations. Since the changes in grain boundary velocities have a strong influence on the evolution of the system, we want to either keep the velocity as a separate variable in the equation or to have the possibility to compute it. In the most general case, we consider a state space $S = \{(l, v, \alpha)\}$, where $l \in \mathbb{R}^+$, $v \in \mathbb{R}$, $\alpha \in (a, b)$.

Our long term goal is to obtain the set of equations describing time evolution of the joint probability density function $\rho(l, v, \alpha)$, the discrete analogue of which up to an appropriate normalization has the form

$$\rho(l, v, \alpha) = \sum_{i,j,k} \delta(l - l_i) \delta(v - v_j) \delta(\alpha - \alpha_k). \quad (2.4)$$

In this study we look at the evolution of the marginal densities

$$\begin{aligned} \rho_{len}(l, t) &= \sum_i \delta(l - l_i), \\ \rho_{vel}(v, t) &= \sum_j \delta(v - v_j), \\ \rho_{or}(\alpha, t) &= \sum_k \delta(\alpha - \alpha_k). \end{aligned}$$

In addition, it is of particular interest for materials science applications to describe the evolution of the lengths ordered by orientations:

$$\rho_w(\alpha, t) = \sum_i l_i(t) \delta(\alpha - \alpha_i),$$

which in the absence of dependence on a normal direction coincides with the grain boundary character distribution. The set of quantities introduced above would completely describe the dynamics of the one-dimensional grain growth model generated by the gradient flow equation (2.2). Moreover, the associated evolution equations, if found, should provide a significant insight into the global problem of texture development in polycrystalline materials microstructure.

3. Simulation statistics. The first step towards a mesoscopic model is the identification of stable statistics. If it turns out that the distributions behave chaotically or fail to stabilize, the analysis will be much more complicated. That is why we undertook the task of simulating the 1-dimensional system described above according to the laws of motion (2.3). The statistics of several numerical experiments for a system of 10000 grain boundaries is presented below. We refer to each grain boundary disappearance event as a simulation "step". Hence, unless there are coincident events, 7000 grain boundaries disappear exactly after 7000 steps.

Figure 3.1 shows evolution of the relative area and relative velocity distributions for the case of a single well potential, which stays approximately the same for other choices of f . Both statistics do not change their shape in the later part of the simulation, however, their spread narrows as time goes on since fewer and fewer grains take part in the statistics. In this figure, the axes are scaled accordingly and we observe the stabilization of both distributions.

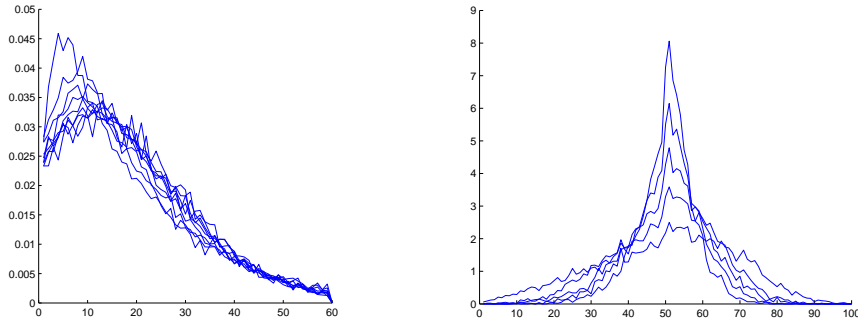


FIG. 3.1. Evolution of marginal pdf for: (a) relative length, (b) relative velocities for $f = (x - 0.5)^2$

In the Figure 3.2 we look at the similar distributions for orientation parameters α for the choice of f having a single or triple minima. The graphs clearly show that the shapes of f and orientations distribution are inversely correlated.

The existence of stable statistics for both length, velocities and orientations motivates the search for a suitable statistical model for this type of dynamics.

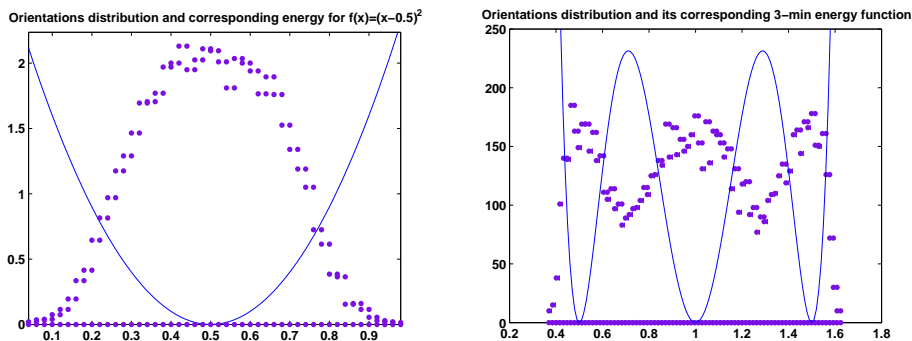


FIG. 3.2. Distribution of the orientations for (a) $f(x) = (x - 0.5)^2$, (b) $f(x) = (x - 0.5)^2(x - 1)^2(x - 1.5)^2$

4. Birth-death model. We will now attempt to derive the evolution equations for the quantities $\rho_{len}(l, t)$ and $\rho_{vel}(v, t)$ based on their interconnection with the distribution of orientations $\rho_{or}(\alpha, t)$. The approach given below is based on the birth-death interpretation of the dynamics of orientations. Indeed, during each critical event some orientations disappear and new orientations develop. In order to quantify the associated birth and death rates, let us introduce the following framework.

We start by introducing relevant quantities and analyzing their relationships.

4.1. Notations and useful relationships. Since it is the energies of α and not orientations themselves that play a role in the dynamics of this system, we will be working with the distribution energies associated to given orientations

$$\rho_f(f(\alpha), t) = \sum_i \delta(f(\alpha) - f(\alpha_i)),$$

rather than ρ_{or} . There is a straightforward relationship between the two. Indeed, recall that for any $f = \sum f_j I(\text{supp}(f_j))$ with strictly monotone and differentiable functions f_j ,

$$\rho_f(f, t) = \sum (\rho_{or} \circ f_j^{-1})(t) / (f_j'(f_j^{-1})(t)),$$

where $I(A)$ is the indicator function of a set A and $\rho_{or}(\alpha, t) = \sum_k \delta(\alpha - \alpha_k)$ is the distribution of orientations. For each monotone part we have

$$\begin{aligned} (\mathbf{E}f)(t) &= \int f(\alpha) \rho_f(f(\alpha), t) df(\alpha) = \\ &= \int f(\alpha) (\rho_{or} \circ f^{-1})[f(\alpha) / (f'(f^{-1})(f(\alpha)))] df(\alpha) = \int f(\alpha) \rho_{or}(\alpha, t) d\alpha. \end{aligned}$$

This corresponds to a change of variables from α to $f(\alpha)$. Let us denote the average of v conditioned on given α as

$$\langle v | \alpha \rangle(t) = \int v' \rho_{vel}(v', t | \alpha) dv'.$$

Notice that the the velocity of the i -th grain boundary with orientation $\alpha = \alpha_i$ is related to the neighboring orientations through

$$v_i(t) = (f(\alpha_{i+1}) - f(\alpha)) + (f(\alpha_{i-1}) - f(\alpha)) = v_1 + v_2.$$

with $v_1 = f(\alpha_{i+1}) - f(\alpha)$ and $v_2 = f(\alpha_{i-1}) - f(\alpha)$. For the purpose of deriving the precise expression for $\langle v | \alpha \rangle(t)$, we have to assume independence of α_i of the neighboring grain boundary orientations α_{i-1} and α_{i+1} . The implications and validity of this assumption will be discussed at the end of this section.

THEOREM 4.1. *If $\alpha = \alpha_i$ is independent of α_{i-1} and α_{i+1} , mean velocity of grain boundaries with orientation α is given by*

$$\langle v | \alpha \rangle(t) = 2 \int [f(\alpha') - f(\alpha)] df(\alpha'). \quad (4.1)$$

Proof. Due to the independence assumption,

$$\rho_{vel}(v, t | \alpha) = \rho_{v_1}(v, t) * \rho_{v_2}(v, t).$$

Since

$$\mathbf{P}(v_1 < v) = \mathbf{P}(f(\alpha_{i+1}) - f(\alpha) < v) = \mathbf{P}(f(\alpha_{i+1}) < f(\alpha) + v)$$

and

$$\mathbf{P}(v_2 < v) = \mathbf{P}(f(\alpha_{i-1}) - f(\alpha) < v) = \mathbf{P}(f(\alpha_{i-1}) < f(\alpha) + v),$$

with $f(\alpha_{i-1})$ and $f(\alpha_{i+1})$ being distributed according to a common density ρ_f , we get

$$\begin{aligned} \rho_{v_1}(v, t) &= \rho_f(f(\alpha) + v, t) \\ \rho_{v_2}(v, t) &= \rho_f(f(\alpha) + v, t). \end{aligned}$$

In other words,

$$\rho_{vel}(v, t|\alpha) = \int \rho_{v_1}(s, t)\rho_{v_2}(v - s, t)ds = \int \rho_f(s + f(\alpha), t)\rho_f(v - s + f(\alpha), t)ds.$$

It follows that

$$\begin{aligned} \langle v|\alpha\rangle(t) &= \int v \left[\int \rho_f(s + f(\alpha), t)\rho_f(v - s + f(\alpha), t)ds \right] dv \\ &= \int \left[\int v\rho_f(v - s + f(\alpha), t)dv \right] \rho_f(s + f(\alpha), t)ds \\ &= \int \left[\int (u + s - f(\alpha))\rho_f(u, t)du \right] \rho_f(s + f(\alpha), t)ds \\ &= \int \left[(\mathbf{E}f)(t) + (s - f(\alpha)) \right] \rho_f(s + f(\alpha), t)ds \\ &= 2[(\mathbf{E}f)(t) - f(\alpha)] \end{aligned}$$

We obtain the following relationship:

$$\langle v|\alpha\rangle(t) = 2 \int [f(\alpha') - f(\alpha)]df(\alpha').$$

□

This has a clear physical interpretation: grain boundaries with interfacial energies higher than current average energy have negative mean velocity, hence tend to shrink, while those with lower energies tend to grow.

4.2. Evolution of orientations in 1d. Let us now turn our attention to the evolution of unweighted α population $\rho_{or}(\alpha, t) = \sum_i \delta(\alpha - \alpha_i)$.

THEOREM 4.2. *Under the assumption of independence of α_i, α_{i-1} and α_{i+1} , the evolution for orientations satisfies*

$$\frac{\partial \rho_{or}(\alpha, t)}{\partial t} = -\rho_{len}(0, t|\alpha)\langle v|\alpha\rangle(t) \quad (4.2)$$

Proof. By computing the impact of "death" events on the overall population of the orientations, we can write

$$\begin{aligned} \rho_{or}(\alpha, t + \Delta t) - \rho_{or}(\alpha, t) &= \{\text{surviving boundaries}\} - \{\text{dead boundaries}\} \\ &= 0 - \sum_{l-v\Delta t \leq 0} \delta(\alpha - \alpha_i) = -P_0(\alpha). \end{aligned}$$

The "death probability" P_0 associated with some fixed α can be computed as follows:

$$\begin{aligned} P_0(\alpha) &= \int \int_{l-v\Delta t \leq 0} \rho_{vel}(v, t|\alpha)\rho_1(l, t|\alpha)dl dv \\ &= \int \rho_{vel}(v, t|\alpha) \int_0^{v\Delta t} \rho_{len}(l, t|\alpha)dl dv \\ &= \int \rho_{vel}(v, t|\alpha) \int_0^{v\Delta t} (\rho_{len}(0, t|\alpha) + l\rho'_{len}(0, t|\alpha))dl dv \\ &= \int \rho_{vel}(v, t|\alpha)(\rho_{len}(0, t|\alpha)v\Delta t + (v\Delta t)^2\rho'_{len}(0, t|\alpha)/2)dv \\ &= \rho_{len}(0, t|\alpha)\langle v|\alpha\rangle(t)\Delta t + 0(\Delta t)^2. \end{aligned}$$

This gives the following evolution equation for the distribution of orientations:

$$\frac{\partial \rho_{or}(\alpha, t)}{\partial t} = -\rho_{len}(0, t|\alpha)\langle v|\alpha\rangle(t)$$

□

4.3. Evolution of grain boundary character distribution in 1d. Analogously, we can derive the evolution of weighted population

$$\rho_w(\alpha, t) = \sum_i l_i(t)\delta(\alpha - \alpha_i),$$

which in one-dimensional case coincides with the sought grain boundary character distribution.

THEOREM 4.3. *Under the assumption of independence of α_i, α_{i-1} and α_{i+1} , the evolution of orientations weighted with relative lengths satisfies*

$$\frac{\partial \rho_w(\alpha, t)}{\partial t} = 2 \left[\int f(\alpha', t)\rho_w(\alpha', t)d\alpha' \right] \rho_w(\alpha, t) - 2f(\alpha, t)\rho_w(\alpha, t) \quad (4.3)$$

Proof.

Similarly to the unweighted case,

$$\begin{aligned} \rho_w(t + \Delta t) - \rho_w(t) &= \{\text{boundaries growing/shrinking}\} - \{\text{dead boundaries}\} \\ &= \sum (l_i(t + \Delta t) - l_i(t))\delta(\alpha - \alpha_i) - \sum_{l-v\Delta t \leq 0} l_i(t)\delta(\alpha - \alpha_i) \\ &= \Delta t \sum v_i(t)\delta(\alpha - \alpha_i) = \Delta t \sum v_i(t)\delta(\alpha - \alpha_i)\delta(v - v_i) \\ &= \Delta t \int v(t)\rho_{vel}(v|\alpha, t)dv = \Delta t \int v(t)\rho_{vel}(v|\alpha, t)\rho_w(\alpha, t)dv \\ &= \Delta t \langle v|\alpha\rangle(t)\rho_w(\alpha, t). \end{aligned}$$

Hence the evolution equation for ρ_w takes on the form

$$\frac{\partial \rho_w(\alpha, t)}{\partial t} = \langle v|\alpha\rangle(t)\rho_w(\alpha, t).$$

Taking into account equation (4.1),

$$\frac{\partial \rho_w(\alpha, t)}{\partial t} = 2 \left[\int (f(\alpha') - f(\alpha, t))\rho_w(\alpha', t)d\alpha' \right] \rho_w(\alpha, t)$$

We can rewrite it in a slightly different form

$$\frac{\partial \rho_w(\alpha, t)}{\partial t} = 2 \left[\int f(\alpha', t)\rho_w(\alpha', t)d\alpha' \right] \rho_w(\alpha, t) - 2f(\alpha, t)\rho_w(\alpha, t)$$

□

Note that it follows from (4.1) that

$$\int \frac{\partial \rho_w(\alpha, t)}{\partial t} d\alpha = \int \langle v(t)|\alpha\rangle \rho_w(\alpha, t) d\alpha = 2 \int (E(f(\alpha, t)) - f(\alpha, t))\rho_w(\alpha, t) d\alpha = 0,$$

as to be expected.

4.4. Evolution of lengths in 1d. Now let us look at $\rho_{len}(l, t) = \sum_i \delta(l - l_i)$.

THEOREM 4.4. *Assuming that diffusion in lengths is a Markov process, its evolution satisfies*

$$\frac{\partial \rho_{len}(l, t|\alpha)}{\partial t} = -\langle v|\alpha \rangle(t) \frac{\partial \rho_{len}(l, t|\alpha)}{\partial l} \quad (4.4)$$

Proof.

Denoting for the moment $\rho(l, t) = \rho_{len}(l, t)$, we can write

$$\begin{aligned} \rho(l, t + \Delta t|\alpha) + o(\Delta t)^2 &= \\ \int \rho(l', t|\alpha) \mathbb{P}(l - l', \Delta t|l', \alpha) dl' &= \int \rho(l - \Delta l, t|\alpha) \mathbb{P}(\Delta l, \Delta t|l - \Delta l, \alpha) d(\Delta l) = \\ \int \left[\rho(l, t) - \frac{\partial \rho}{\partial l} \Delta l + \frac{1}{2} \frac{\partial^2 \rho}{\partial l^2} (\Delta l)^2 \right] \times \left[\mathbb{P}(\Delta l, \Delta t|l) - \frac{\partial \mathbb{P}}{\partial l} \Delta l + \frac{1}{2} \frac{\partial^2 \mathbb{P}}{\partial l^2} (\Delta l)^2 \right] d(\Delta l) &= \\ \rho(l, t|\alpha) - \frac{\partial \rho(l, t|\alpha)}{\partial l} \langle \Delta l|\alpha \rangle + \frac{1}{2} \frac{\partial^2 \rho(l, t|\alpha)}{\partial l^2} \langle \Delta l^2|\alpha \rangle - & \\ \rho \cdot \frac{\partial \langle \Delta l|\alpha \rangle}{\partial l} + \frac{\rho}{2} \frac{\partial^2 \langle \Delta l^2|\alpha \rangle}{\partial l^2} + \frac{\partial \rho}{\partial l} \frac{\partial \langle \Delta l^2|\alpha \rangle}{\partial l} &= \\ \rho(l, t|\alpha) - \frac{\partial}{\partial l} \left[\rho(l, t|\alpha) \langle \Delta l|\alpha \rangle \right] + \frac{1}{2} \frac{\partial^2}{\partial l^2} \left[\rho(l, t|\alpha) \langle \Delta l^2|\alpha \rangle \right] & \end{aligned}$$

In other words,

$$\frac{\partial \rho(l, t|\alpha)}{\partial t} = -\frac{\partial c_1 \rho(l, t; \alpha)}{\partial l} + \frac{1}{2} \frac{\partial^2 c_2 \rho(l, t|\alpha)}{\partial l^2}, \text{ where } c_1 = \frac{\langle \Delta l|\alpha \rangle}{\Delta t}, c_2 = \frac{\langle \Delta l^2|\alpha \rangle}{\Delta t}$$

Notice that since $\Delta l = \langle v \rangle \Delta t$, $\langle \Delta l \rangle = \langle v \rangle \Delta t = 0$ and so $\langle v \rangle = 0$. It follows that $c_1 = \frac{\langle \Delta l|\alpha \rangle}{\Delta t} = \langle v|\alpha \rangle$ and $c_2 = \frac{\langle \Delta l^2|\alpha \rangle}{\Delta t} = \langle v|\alpha \rangle^2 \Delta t \rightarrow 0$ as $\Delta t \rightarrow \infty$, so that

$$\frac{\partial \rho_{len}(l, t|\alpha)}{\partial t} = -\langle v(t)|\alpha \rangle \frac{\partial \rho_{len}(l, t|\alpha)}{\partial l}$$

This equation integrated in l yields (4.3), as to be expected. \square

According to this model, if we assume independence of neighboring orientations, we get a drift term related to the mean velocity of the grain boundaries conditioned on their orientations and the diffusion part becomes negligible.

4.5. Numerical results. This regime is a special case of the Fokker-Planck kinetic equations, which agrees well with the conservation laws and has very good agreement with numerical results at the beginning of the simulation, as shown in Figures 4.1, 4.2.

However, it tends to deviate from the exact solution as time grows, as shown in Figure 4.3. This points out to possible growth of dependence between the neighboring α populations, that have a tendency to cluster according to their minimum misorientations. These observations led to the development of a statistical mechanics approach that is described in the next Chapter.

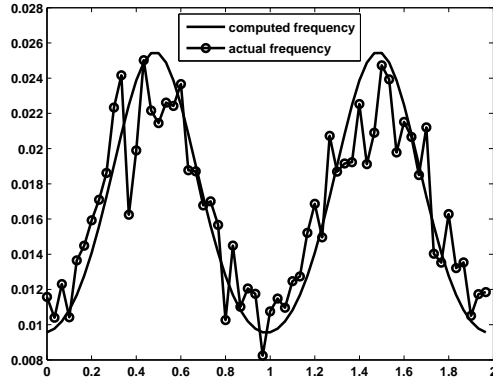


FIG. 4.1. Illustration of the agreement of distributions at the initial stages of the evolution. Distribution of orientations produced by the PDE compared to the simulation for $f = (x - 0.5)^2(x - 1.5)^2$.

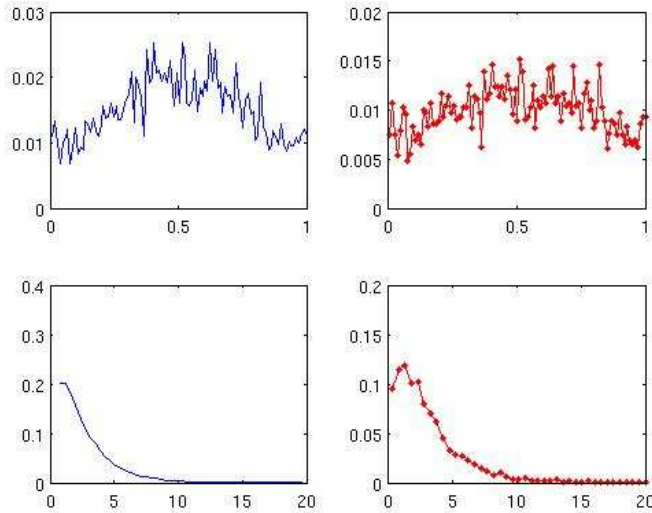


FIG. 4.2. Illustration of the agreement of distributions at the initial stages of the evolution. Distribution of orientations (top figures) and lengths (bottom figures) produced by the PDE (left) compared to the simulation (right) for $f = \cos(2\pi x) + 1$.

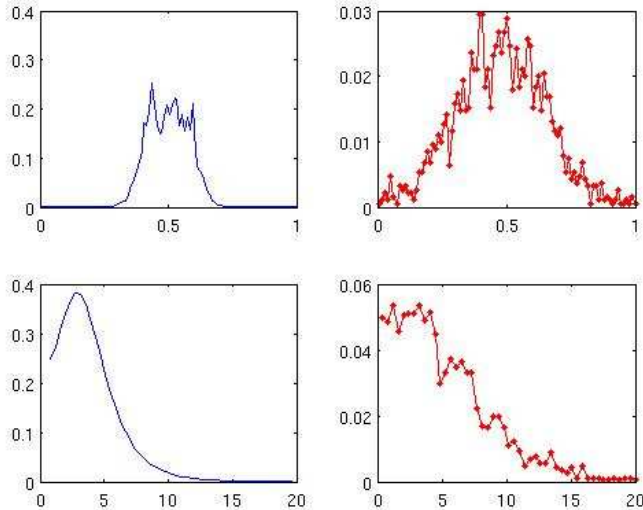


FIG. 4.3. Illustration of departure from initial agreement in later stages of the evolution. Distribution of orientations (top figures) and lengths (bottom figures) produced by the PDE (left) compared to the simulation (right) for $f = \cos(2\pi x) + 1$.

5. Boltzmann-type kinetic equation.

5.1. Reduced space model. Here we will focus our attention on the view adopted from the theory of gas dynamics [13],[12]. More precisely, we can regard our system of grain boundaries (intervals) as a collection of interacting particles moving with velocities v_i . Each particle has parameters (l_i, α_i) , where $\dot{l}_i = v_i$. Notice that in contrast with the statistical mechanics approach, we do not intend to keep positions of the grains as part of the equation, since otherwise we run into the risk of reducing the benefits the present approach may have for all practical grain growth applications. This fact, however, has an added cost of making further modeling of the system more complicated. Nevertheless, we might still be able to write down the exact rules of collision and corresponding kinetic equations.

Indeed, observe that in these variables each collision event is completely determined by the pair of values (v, α) for each of the interacting grain boundaries. For example, during the collapse of a grain boundary (v_2, α_2) , its neighbor (v_1, α_1) acquires the new velocity according to the rule

$$v^* = v_1 + v_2 + f(\alpha_2) - f(\alpha_1), \quad (5.1)$$

while the orientation parameter α_1 remains unchanged. This way the intrinsic correlations between the neighbors get preserved through the velocity expression $v = f(\alpha_{i+1}) + f(\alpha_{i-1}) - 2f(\alpha)$, as is necessary for producing correct dynamics due to the reasons mentioned above. It can be worthwhile to note that this kind of collision dynamics resembles the case of a "sticky" collision of completely inelastic particles observed, for example, in granular gases, as described in [14].

Next, we can write the continuity equation for the density function $\rho(l, v, \alpha, t)$,

arriving at the following form of the equation of motion:

$$\frac{\partial \rho(l, v, \alpha, t)}{\partial t} + v \frac{\partial \rho(l, v, \alpha, t)}{\partial l} = \left[\frac{\partial \rho(l, v, \alpha, t)}{\partial t} \right]_c \quad (5.2)$$

Here the term on the right hand side accounts for the interchange in the populations (the rate of change in the density) due to collisions.

$$\left[\frac{\partial \rho(l, v, \alpha, t)}{\partial t} \right]_c = \{gain\} - \{loss\} \quad (5.3)$$

Similarly to the derivation of the inelastic Boltzmann equation, this term can be written as an integral over all possible collisions:

$$\begin{aligned} \frac{\partial \rho(l, v, \alpha, t)}{\partial t} + v \frac{\partial \rho(l, v, \alpha, t)}{\partial l} = \\ \frac{1}{N^2(t)} \int \int \int v_0 \rho(0, v_0, \alpha_0, t) \rho(l, v', \alpha', t) [\delta(v - v^*) - \delta(v - v')] dv' dv_0 d\alpha_0 \end{aligned} \quad (5.4)$$

with $v^* = v' + v_0 + f(\alpha_0) - f(\alpha)$ being the new velocity for the collided grain boundary and $N(t)$ denoting the total number of boundaries at time t .

Here $v_0 \rho(0, v_0, \alpha_0, t) \rho(l, v', \alpha', t) / N^2(t)$ is the collision rate under the assumption of reasonable independence of (l, v, α) populations. The difference of Dirac delta functions denotes the gain and loss of grain boundaries within each population during a collision.

Notice that by integrating this equation over all possible velocities, we get back our earlier advection equation (4.4), so this approach represents a natural extension of the mean velocity theory based on orientations presented earlier.

The simulation of this equation showed that this approach gives good agreement with the actual simulation for some period of time, after which it becomes impossible to find the right pair of colliding grain boundaries. In other words, the equation $v_0 + 2f(\alpha_0) = f(\alpha') + f(\alpha'')$ for the dying grain boundary (α_0, v_0) with interacting neighbors (α', v') , (α'', v'') becomes inconsistent by violating $v_0 + 2f(\alpha_0) \geq 0$. The reason behind it is that by picking random neighbors uniformly we leave too much freedom in the motion of the particles, which eventually takes us to a wrong grain configuration. Another way to express this is that the molecular chaos assumption does not seem to hold in this state space.

To suppress the freedom of motion, we should get rid of the chaotic behavior in the first level of neighboring grains. This can be done either by imposing some strict conditions on the choice of grain boundaries participating in each collision or by further extending the state space of the model to include a first level of dependencies. As part of the first approach, we considered the following set of restricting conditions:

1. $v' < 0$
2. $f(\alpha') < f(\alpha_0)$
3. $v_0 + f(\alpha_0) - f(\alpha') \leq 0$
4. $v' + v_0 + f(\alpha_0) + f(\alpha') \geq 0$

which extended the lifetime of the system but not significantly. It remains an open question whether there might exist another set of conditions that can be imposed on the system to correct this flaw. Since the observations of model behavior in the initial period of time showed very good agreement with the actual simulation, there is a reason to believe that the model would work well if it is allowed to run for a longer period of time.

The major obstacle in using this approach lies in the increased computational complexity associated with evaluating triple integrals in (5.4). Indeed, we have found that a simple Matlab routine has to be replaced by a faster C-version in order to produce 10000 grain collision dynamics in reasonable time frame. There is a reason to believe, however, that this complexity can go down, not up, in the case of higher dimensional problems, since additional freedom of movement will contribute positively to the validity of the model and may lead to a simpler estimate for the collision rates.

5.2. Extended state space model. As an alternative, we can split the grain boundary velocity into 2 parts v_l and v_r , for the left and the right endpoint separately:

$$\rho(l, v_l, v_r, \alpha, t)$$

Let x_l and x_r are the endpoints and the α_l and α_r are the left and right neighbors of the grain boundary with orientation α and length l . In terms of variables (l, v_l, v_r, α, t) , we can always find the left and right neighbors by solving the equations

$$f(\alpha_l) = f(\alpha) - v_l, \quad f(\alpha_r) = f(\alpha) + v_r$$

where $dx_l/dt = v_l = f(\alpha) - f(\alpha_l)$ and $dx_r/dt = v_r = f(\alpha_r) - f(\alpha)$. Then the jumps in the velocities for the neighbors of the dying grain boundary α can be written as:

$$v_r(\alpha_l) = v_l(\alpha_r) = v_l(\text{dead}) + v_r(\text{dead})$$

In simple words, it means that the velocities of two colliding boundaries add up during the collision. By following these simple collision rules, we can write another Boltzmann-type collision equation for the density function:

$$\frac{\partial \rho(l, v_l, v_r, \alpha, t)}{\partial t} + (v_r - v_l) \frac{\partial \rho(l, v_l, v_r, \alpha, t)}{\partial l} = \left[\frac{\partial \rho(l, v_l, v_r, \alpha, t)}{\partial t} \right]_c \quad (5.5)$$

where

$$\begin{aligned} \left[\frac{\partial \rho(l, v_l, v_r, \alpha, t)}{\partial t} \right]_c &= \int (v_l - 2v'_l) \rho(0, v'_l, v_l - v'_l, \alpha_l, t) dv'_l \\ &+ \int (2v'_r - v_r) \rho(0, v_r - v'_r, v'_r, \alpha_r, t) dv'_r \\ &- \int (v_l - v'_l) \rho(0, v'_l, v_l, \alpha_l, t) dv'_l \\ &- \int (v'_r - v_r) \rho(0, v_r, v'_r, \alpha_r, t) dv'_r \end{aligned} \quad (5.6)$$

This equation can be written in an equivalent form in terms of $(l, \alpha, \alpha_l, \alpha_r)$ instead of velocities.

We have inflated the dimension of the problem by introducing neighboring grain information into the distribution function. This may lead to a significant increase of complexity if the model is extended to higher dimensions. Note, however, that the nearest neighbor correlations observed in this one-dimensional model are expected to become weaker as the topology of the problem changes, since the pool of interacting triple junctions will get a new random supply of orientations not present when we restrict ourselves to a line.

The results of the extended model as expected agree perfectly with the actual simulation and remain valid until the very last stage of the simulation, as outlined in Figure 5.1. We have found numerical Monte-Carlo integration approach provides a very nice performance to this model.

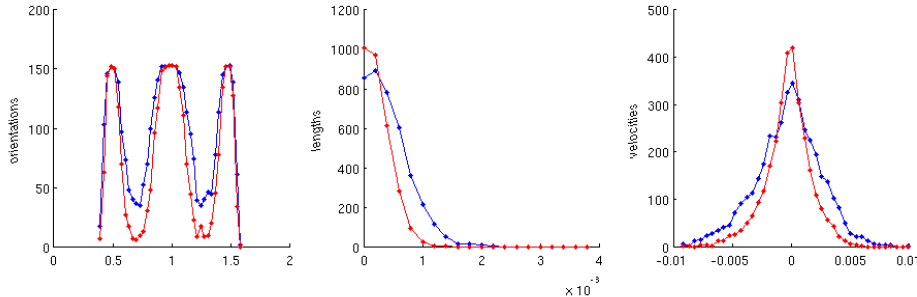


FIG. 5.1. Comparing orientations (left), lengths (center) and velocities (right) distributions for the simulation (red) and the MC-version of the birth-death density evolution equation for the 3 minima case.

Compared to the reduced model, equation (5.6) gives a much better agreement with the actual data, but it does require a lot more parameters. While this is not crucial in the 1-dimensional example considered here, it will surely lead to complications when we take into account all neighboring grains in the real two- or three-dimensional data. According to the remarks made earlier, however, the reduced space collision dynamics should provide a more reasonable approximation once the unrealistic restrictions posed by the problem topology are removed.

6. Discussion. We have presented two frameworks for modeling critical events in microstructure evolution and analyzed their capabilities by applying them to a simplified model specifically designed to target the evolution of triple junctions during grain growth disregarding mean curvature effects present in the real systems. One model is based on the birth-death description motivated by the idea of averaging over segments with common orientation. This approach fits well within several traditional and more recent theories for anisotropy and has a good potential for explaining the relation between grain boundary character distribution and underlying interface energy. Another approach is motivated by the theory of sticky gas dynamics. It has a capability to model critical events more thoroughly through the set of collision rules and hence goes beyond the averaging ideas used in the birth-death model.

Both approaches proved to be effective in the early stages of the simulation. We have discovered, however, that a significant correlation develops in this 1-dimensional problem between neighboring orientations after about half of the segments have disappeared, which hinders the performance of both approaches. One possible remedy to this problem proposed in this work is the extended space Boltzmann equation that takes into account all local reconfigurations in the grain boundary network and successfully reproduces the distributions during full system lifecycle. This approach leads to an expansion of the problem state space for higher dimensional problems. However, there is a reason to believe that correlations will be much weaker in higher dimensions after removal of the topological constraints associated with the one-dimensional model, in which case state expansion might be avoided. The magnitude of the effect correlations have on the grain boundary network in higher dimensions is currently under investigation. Its implications on the theories presented above will be the subject of future publications.

7. Acknowledgment. The support by the Center for Nonlinear Analysis (CNA) under the National Science Foundation Grant No. 0405343 is gratefully acknowledged. The work of David Kinderlehrer was also supported by the MRSEC (CMU) under grants DMS-0305794 and DMR-0520425. Dmitry Golovaty wishes to acknowledge grant number DMS-0407361.

REFERENCES

- [1] Mellars, P., "Going East: New Genetic and Archaeological Perspectives on the Modern Human Colonization of Eurasia", *Science*, 313, p. 796 - 800, 2006
- [2] Mullins, W. W., "A One Dimensional Nearest Neighbor Model of Coarsening", *Proceedings of the Calculus of Variations and Nonlinear Material Behavior*, Carnegie Mellon University, 1990
- [3] Mullins, W.W., "Two-dimensional Motion of Idealized Grain Boundaries", *J. Appl. Phys.*, 27, pp. 900-904, 1956.
- [4] Mullins, W.W., "Solid Surface Morphologies Governed by Capillarity, Metal Surfaces: Structure, Energetics, and Kinetics", ASM, Cleveland, 1963
- [5] S. Agmon, A. Douglis and L. Nirenberg, "Estimates near the boundary for solutions of elliptic partial differential equations satisfying general boundary conditions", II, *Comm. Pure Appl. Math.*, 17, 3592 1964.
- [6] L. Bronsard and F. Reitich, "On three-phase boundary motion and the singular limit of a vector-valued Ginzburg-Landau equation", *Arch. Rat. Mech. Anal.* 124, pp. 355-379, 1993.
- [7] Kinderlehrer, D., Livshits, I., Rohrer, G.S., Ta'asan, S., and Yu, P., "Mesoscale evolution of the grain boundary character distribution, Recrystallization and Grain Growth", *Materials Science Forum*, vols. 467-470, pp. 1063-1068, 2004
- [8] Kinderlehrer, D., Livshits, I., Manolache, F., Rollett, A. D., and Ta'asan, S., "An approach to the mesoscale simulation of grain growth", *Influences of interface and dislocation behavior on microstructure evolution*, (Aindow, M. et al., eds), *Mat. Res. Soc. Symp. Proc.* 652, Y1.5., 2001
- [9] V.E. Fradkov, D. Udler, "Two-dimensional normal grain growth: topological aspects", *Advances in Physics*, Vol.43, No.6, 739-789, 1994
- [10] H.V. Atkinson, "Theories on normal grain growth in pure single phase systems", *Acta Metall.*, Vol. 36, No.3, p.469-491, 1988
- [11] M. Emelianenko, D. Golovaty, D. Kinderlehrer, S. Taasan, "Texture evolution via continuous time random walk theory", *Center for Nonlinear Analysis*, No. 06-CNA-011, 2006
- [12] Anna de Masi, Enrico Presutti, "Mathematical Methods for Hydrodynamic Limits", Springer-Verlag, 1991
- [13] Ludwig Boltzmann, "Lectures on gas theory", Dover 1995
- [14] D. Benedetto, E. Caglioti, M. Pulvirenti, "A kinetic equation for granular media", *Math. Mod. and Num. An.*, 31 n. 5, pp 615-641, 1997